Project 058 Improving Policy Analysis Tools to Evaluate Higher-Altitude Aircraft Operations

Massachusetts Institute of Technology

Project Lead Investigator

Steven R. H. Barrett
Professor of Aeronautics and Astronautics
Director, Laboratory for Aviation and the Environment
Massachusetts Institute of Technology
77 Massachusetts Ave, Building 33-322, Cambridge, MA 02139
617-452-2550
sbarrett@mit.edu

Sebastian D. Eastham
Research Scientist
Laboratory for Aviation and the Environment
Massachusetts Institute of Technology
77 Massachusetts Ave, Building 33-322, Cambridge, MA 02139
617-253-2170
seastham@mit.edu

University Participants

Massachusetts Institute of Technology (MIT)

- P.I.: Prof. Steven R. H. Barrett
- FAA Award Number: 13-C-AJFE-MIT, Amendment Nos. 064, 089, and 099
- Period of Performance: February 5, 2020 to September 19, 2023
- Reporting Period: October 1, 2021 to September 30, 2022
- Tasks (Note: tasks completed before this reporting period are listed as completed):
    1. Develop a set of emissions scenarios for high-altitude aviation
    2. Extend and validate MIT's existing atmospheric simulation capabilities (completed)
    3. Simulate atmospheric impacts of high-altitude emissions by using updated capabilities
    4. Calculation of atmospheric sensitivity matrices
    5. Develop and update operational tools capable of quantifying environmental impacts of aviation
    6. Regionalized contrail parameterization
    7. Investigate the dependence of aviation emissions impacts on non-aviation factors

Project Funding Level

This project received $1,150,000 in FAA funding and $1,150,000 in matching funds. Sources of match are approximately $218,000 from MIT, plus third-party in-kind contributions of $391,000 from NuFuels, LLC, $127,000 from Savion Aerospace Corporation, and $414,000 from Google, LLC.

Investigation Team

Principal Investigator:	Prof. Steven Barrett (MIT) (all tasks)
Co-Principal Investigator:	Dr. Sebastian Eastham (MIT) (all tasks)
Postdoctoral Researcher:	Dr. Sadia Afrin (MIT) (all tasks)
Graduate Research Assistants:	Lucas Jeongsuk Oh (MIT) (Tasks 1, 3, and 4)
	Joonhee Kim (MIT) (Tasks 4–6)
	Carla Grobler (MIT) (Task 7)
	Prakash Prashanth (MIT) (Task 7)

Project Overview

Companies are proposing, developing, and testing aircraft operating at higher altitudes, such as commercial supersonic aircraft and high-altitude, long-endurance unmanned aerial vehicles. These aircraft offer the potential to enable new use cases and business models in the aviation sector. However, the combustion emissions of these vehicles will have atmospheric impacts that differ from those of conventional subsonic aviation, because of the higher altitudes of emission. Emissions at higher altitudes are associated with a different chemical environment, longer emissions lifetimes, and transport of emissions over greater distances. Furthermore, new developments in emissions impact estimation have provided a more nuanced view of the environmental consequences of conventional aircraft activity, including the recognition that their climate and air quality impacts both vary depending on the prevailing conditions of the emissions and the time horizon of the assessment.

In this project, we propose to quantify the environmental consequences of such high-altitude aviation emissions. For this purpose, we will perform high-fidelity atmospheric simulations by further developing and applying the GEOS-Chem UCX tropospheric–stratospheric chemistry–transport model and its adjoint. The results will be leveraged to (a) evaluate the climate (radiative forcing; RF) effects of high-altitude aircraft emissions, and (b) estimate the sensitivity of the global ozone column and surface air quality to these emissions. Consequently, the climate, air quality, and ozone impacts for a small number of different proposed supersonic aircraft designs and performance characteristics will be quantified. We will also perform a historical assessment of the impacts of aviation emissions, quantifying how factors such as changing emissions indices and an evolving chemical background have affected—and will affect—the total impacts. On the basis of data from these simulations, a flexible, rapid approach for assessing the impacts of sub- and supersonic aircraft will be presented.

Task 1 - Develop a Set of Emissions Scenarios for High-Altitude Aviation

Massachusetts Institute of Technology

Objective

This task is aimed at developing emissions inputs that cover scenarios relevant to near-future aviation, extending impact estimation to cover a range of altitudes exceeding those of current commercial airline activities. The specific focus of the work during this period was to test and refine the developed global supersonic emissions inventories.

Research Approach

The team continued to develop a mathematical model able to produce an estimate of emissions of key chemical species (e.g., nitrogen oxides (NO_x), sulfur oxides (SO_x), water vapor, black carbon, and organic carbon) during the reporting period. In the meantime, deficiencies were found and corrected. In particular, the previously developed MIT scenarios evaluated the market too conservatively with respect to the scenario designed in ASCENT 10, thus resulting in a significant difference in the amounts of emissions by the supersonic fleet. Therefore, new emissions scenarios were developed on the basis of the assumption that the market status of the supersonic fleet is high, low, or intermediate, to strengthen the capabilities of our research. This diversification of the emissions scenarios not only allows us to predict the demand for the future supersonic fleet for each demonstrated situation, but also expands the predictability and capabilities of our tool.

The fuel burn emissions maps corresponding to each scenario are shown in Figure 1. In the MIT High case, the market need for supersonic aviation has high growth, the MIT Low case reflects low economic growth, and the MIT Mid case is intermediate between the MIT High and MIT Low cases. The difference between the MIT Low and MiT High cases is reflected in underlying market demand; however, the flight frequency does not simply increase for the same overall flight network. As the market expectation increases, flight frequency can increase but new routes can also be established for supersonic travel. The base supersonic aircraft fleet to be assessed was designed through prior research under ASCENT 58, a previous NASA-funded project, and additional information from ASCENT 47.

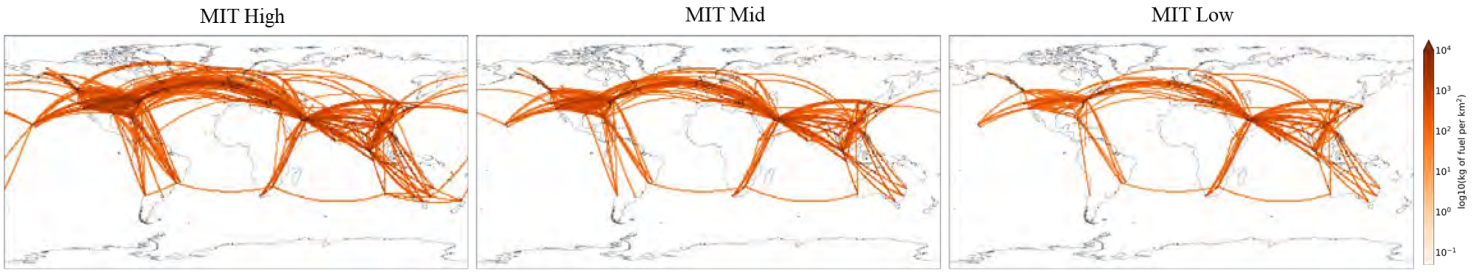

Figure 1. Emissions maps for representative supersonic aircraft developed at MIT. Left: MIT High; middle: MIT Mid; right: MIT Low.

In addition to using the emissions inventory developed by ASCENT 58, our team used an emissions scenarios from ASCENT 10. Using emissions scenarios produced in other studies helps to ensure that the model is robust. In particular, our team can verify our tools' capabilities and increase the reliability of the results through exchanges with the research group conducting environmental analysis by using the ASCENT 10 data. Therefore, we also interacted with the ASCENT 22 team in the emissions inventory we produced.

The tool developed under ASCENT 58 expects data to be converted to a common resolution. This requires solving two problems, which were explored in the process of preparing emissions data from ASCENT 10. First, a difference existed between the resolution of the tool used by ASCENT 10 and that used by our tools. The second problem was that a naïve application of segmented data (as provided by ASCENT 10) results in discontinuities in the emission grid. Therefore, we recognized a need to develop an algorithm to change any resolution to fit the dimension requirements of our tool and developed an algorithm to solve the two problems described above—the discrepancy in resolution and discontinuity.

To solve the discontinuity problem, we used a method of splitting discrete points into smaller pieces than the minimum grid size of the target resolution. This method calculated all values at designated points through 3D linear interpolation (latitude, longitude, and height) among discontinuously distributed locations along the flight path. Therefore, data arranged in tiny grids needed to be redistributed according to the targeting resolution to resolve the disparity in resolution. To this end, we cut the atmosphere in advance according to the target resolution (i.e., a large grid), then calculated the value corresponding to the target resolution grid by counting the small grid in a large grid and adding all emission elements inside it. Ultimately, we verified the law of mass conservation before and after conversion to determine whether any abnormalities were present. The changes in emissions before and after algorithm conversion are shown in Figure 2.

Figure 2. Emissions maps for representative supersonic aircraft developed by ASCENT 10 before and after conversion. Left: before the conversion; right: after the conversion.

We compared and analyzed the results developed by ASCENT 10 and ASCENT 58. When compared with ASCENT 10, ASCENT 58 has more conservative market expectations, and our team predicted that fewer supersonic fleet flights would occur in the target year. Our team also has an estimate of 2035 subsonic flights. Table 1 summarizes overall design choice and emissions characteristics under the three scenarios in ASCENT 58, one scenario provided in ASCENT 10, and the 2035 subsonic flight.

Table 1. Design information and emissions characteristics of supersonic fleets for each emissions inventory (Georgia Institute of Technology [Georgia Tech] case from ASCENT 10; MIT cases from ASCENT 58 and ASCENT 4; and subsonic 2035 case)

	Emissions cases				
	Georgia Tech	**MIT High**	**MIT Mid**	**MIT Low**	**Subsonic 2035**
Mach number	2.2	1.6	1.6	1.6	-
Passenger capacity	55	100	100	100	-
Maximum range, nmi	4,500	3,500	3,500	3,500	-
Cruise ceiling, km	21	17	17	17	12
Fuel per 100 seat-km, kg/100 seat-km	19.0	7.15	7.13	7.08	2.26
Total fuel burn, Tg	122	43.1	19.3	9.56	424
Fleet average EINO_x, g/kg-fuel	14.7	9.05	9.05	9.18	15.2
Total NO_x, Gg ($GgNO_2$ equivalent)	1800	390	175	87.8	6440
Total black carbon, Gg	6.12	1.36	0.607	0.300	34.8
Fuel sulfur content, ppm	600	600	600	600	600
Fleet average EIH_2O, kg/kg-fuel	1.231	1.231	1.231	1.231	1.231

We also conducted a detailed analysis of the information provided by ASCENT 10 and the information developed by our team. The emissions by altitude and latitude were calculated for more detailed analysis and comparison. The ASCENT 10 team projected that approximately 83% of emissions would be allocated to the northern hemisphere (NH). In contrast, our team projected that approximately 91% of emissions would occur in the NH. More specifically, we projected that 57% of emissions would occur between 30˚ and 60˚ latitude, whereas ASCENT 10 projected 38%. Because of the difference in cruise ceiling altitude, the altitude at which the greatest emissions occur is also different.

The attitude at which the greatest emissions occur is the 19–21 km band for the ASCENT 10 inventory, compared to 16-18 km for the MIT inventory (see Figure 3). This is a useful difference, as we can rigorously assess the response simulated in the ASCENT 58 tool for multiple cruise altitude scenarios.

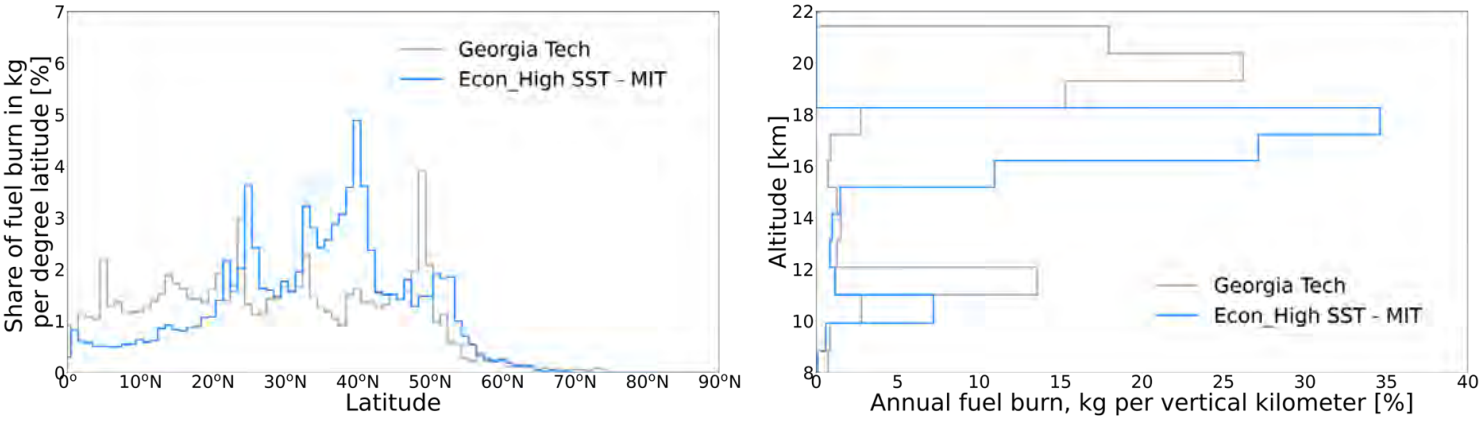

Figure 3. Share of fuel burn distribution. Left: annual fuel burn distribution by latitude; right: by altitude.

Milestones

- New emissions maps for representative supersonic aircraft were generated (Figure 1).
- The ASCENT 10 data were transformed into continuous data and modified for use in the MIT simulation tool (Figure 2).
- The characteristics of the scenarios developed by ASCENT 58 and ASCENT 10 were analyzed (Table 1 and Figure 3).

Major Accomplishments

- The team developed new emissions scenarios assuming high-activity market status.
- New developed emissions inventories were provided to ASCENT Project 22 to enable comparison of estimated impacts by using multiple models.
- The team developed an algorithm that can modify the entire dimensions and continuity of the data even if the data formats differ. The ASCENT 10 data were changed to align with those of ASCENT 58 with the algorithm (Figure 2).

Publications

None.

Outreach Efforts

Progress on all tasks was communicated during biweekly briefing calls with the FAA and reported in quarterly progress reports. ASCENT project 58 was also the subject of a report delivered to the 2022 ASCENT Fall Meeting.

Awards

None.

Student Involvement

During the reporting period of academic year (AY) 2021–2022, the MIT graduate student involved in this task was Lucas Jeongsuk Oh.

Plans for Next Period

Task 1 was largely completed in AY 2021–2022. The team will continue testing, refining, and comparing the global emissions data sets in AY 2022–2023.

Task 2 - Extend and Validate MIT's Existing Atmospheric Simulation Capabilities

Massachusetts Institute of Technology

Objective

The objective of Task 2 is to extend and validate MIT's existing atmospheric simulation capabilities, with the specific goal of ensuring that impacts on critical metrics of air quality and climate can be accurately represented. During AY 2020–2021, the team developed and tested a higher-resolution version of the GEOS-Chem UCX tropospheric–stratospheric global chemistry–transport model to capture localized effects.

Research Approach

The team is using the GEOS-Chem UCX tropospheric–stratospheric global chemistry–transport model as the central tool to quantify climate, air quality, and ozone impacts resulting from high-altitude aviation (Eastham et al., 2014). Therefore, the capabilities of this model for these purposes must be evaluated, and those capabilities must be extended where necessary. Two major subtasks have been identified: Task 2a, increasing the resolution of the model to capture localized impacts at a global resolution of 2°×2.5° or equivalent; and Task 2b, implementing a technique to estimate stratospherically adjusted RF, rather than instantaneous RF. Task 2b was largely completed in AY 2019–2020, whereas Task 2a work was completed in AY 2020–2021. Details of this task have been provided in prior annual reports.

Milestones

Task 2 was completed in AY 2020–2021.

Major Accomplishments

A manuscript was published that used the new stratospherically adjusted RF calculations to evaluate the impacts of supersonic civil aviation on the environment.

Publications

Eastham, S. D., Fritz, T., Sanz-Morère, I., Prashanth, P., Allroggen, F., Prinn, R. G., Speth, R. L., & Barrett, S. R. H. (2022). Impacts of a near-future supersonic aircraft fleet on atmospheric composition and climate. *Environmental Science: Atmospheres*, *2*(3), 388–403. Doi: 10.1039/D1EA00081K

Outreach Efforts

Progress on all tasks was communicated during biweekly briefing calls with the FAA and reported in quarterly progress reports.

Awards

None.

Student Involvement

None.

Plans for Next Period

Task 2 was completed in AY 2020–2021.

References

Eastham, S. D., Weisenstein, D. K., & Barrett, S. R. H. (2014). Development and evaluation of the unified tropospheric–stratospheric chemistry extension (Ucx) for the global chemistry-transport model GEOS-Chem. *Atmospheric Environment*, *89*, 52–63. Doi: 10.1016/j.atmosenv.2014.02.001

Task 3 - Simulate Atmospheric Impacts of High-Altitude Emissions by Using Updated Capabilities

Massachusetts Institute of Technology

Objective

The objective of this task is to estimate the atmospheric response to the representative near-future aviation scenarios described in Task 1, and to convert the raw model outputs to impacts. These simulations will calibrate the simulated impacts and the performance of the new version of the Aviation environmental Portfolio Management Tool–Impacts (APMT-IC).

Research Approach

To achieve the goal of Task 3, the team plans to conduct simulations for more than 10 years. During this reporting period, simulations for a total of 3 years were executed with further simulations ongoing.

Our team plans to ultimately include all chemical species (NO_x, SO_x, water vapor, black carbon, organic carbon, and unburned hydrocarbons) to estimate the atmospheric response to supersonic aviation. The focus thus far has been on NO_x which was identified as the priority pollutant, excluding other pollutants for the purpose of initial evaluation. We therefore simulate three years of impacts for supersonic aircraft NO_x emissions from three different fleets as previously described.

First, the baseline case underlying all simulations was set. The baseline assumed a point at which no future supersonic aviation would occur. Our team updated the subsonic aviation with the estimate for the year 2035 and included the estimation in the baseline to increase credibility. Thus, we created a test case that adds a supersonic fleet case to the baseline. In this way, we determined the degree of the environmental impact of near-future aviation scenarios by subtracting the environmental response obtained through baseline from the results obtained through the test case.

Specific outcomes investigated for each scenario are changes in the global ozone column and in surface air quality, including ozone and fine particulate matter ($PM_{2.5}$). These results were calculated at a global resolution of 2˚×2.5˚ (see Task 2) by using GEOS-Chem (including the UCX stratospheric chemistry capabilities). These outcomes were estimated by forward sensitivity analysis in Task 4. Figure 4, Figure 5, and Figure 6 show the simulation results for the third year. Each result is an environmental change caused by the supersonic fleet.

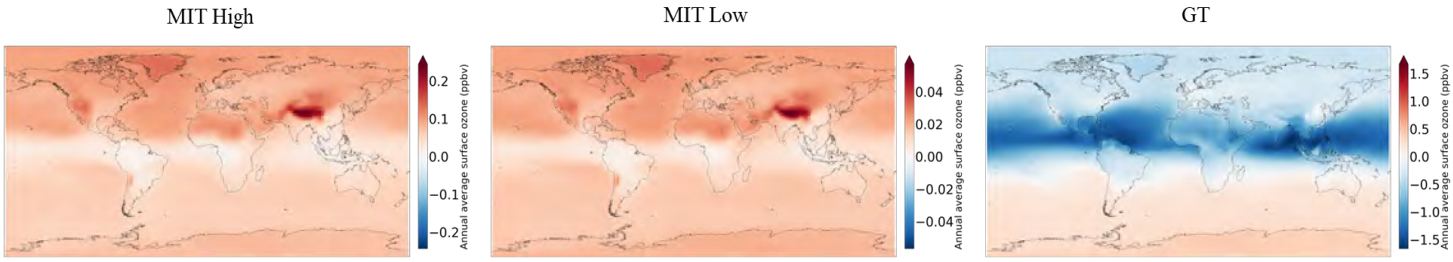

Figure 4. Changes in annual mean surface ozone concentrations due to SST emissions from three scenarios after 3 years. Left: MIT High; middle: MIT Low; right: Georgia Tech (ASCENT 10).

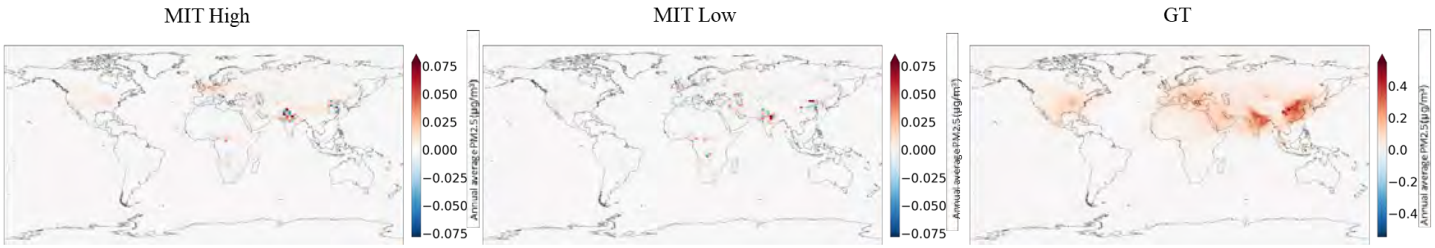

Figure 5. Changes in annual mean surface $PM_{2.5}$ concentrations due to SST emissions from three scenarios after 3 years. Left: MIT High; middle: MIT Low; right: Georgia Tech (ASCENT 10).

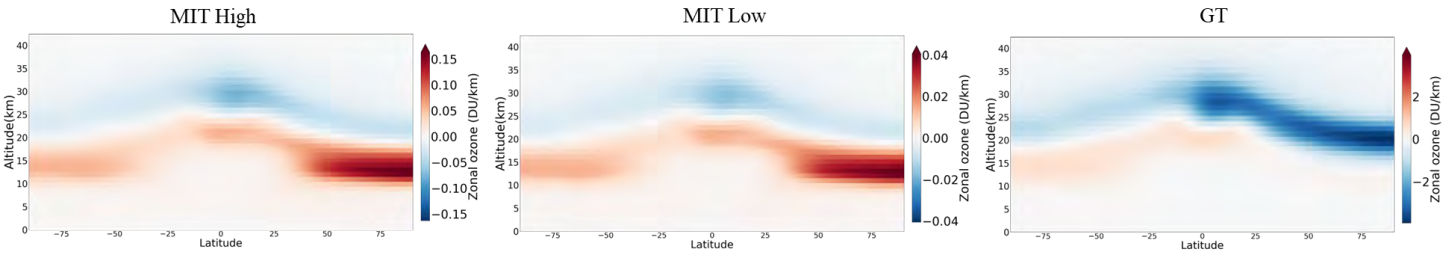

Figure 6. Changes in zonal mean ozone concentrations due to SST emissions from three scenarios after 3 years. Left: MIT High; middle: MIT Low; right: Georgia Tech (ASCENT 10). DU/km = Dobson units per vertical kilometer.

The simulated impacts of emissions differ for the different fleets. Surface ozone increases in response to the MIT cases but decreases in response to the Georgia Tech/ASCENT 10 case, because the cruise flight altitude in the case of Georgia Tech is higher than that of MIT. This is also the cause of the different pattern of ozone change (Figure 6). Meanwhile the pattern of change is nearly identical for MIT High and MIT Low, reflecting the relative linearity of the response for emissions at the same altitude. In addition, because the Georgia Tech case emits more NO_x than the MIT case, the resulting increase in $PM_{2.5}$ is greater.

Milestones

- Full forward GEOS-Chem simulations at high resolution (2°×2.5°) to quantify the climate, ozone, and air quality response to representative supersonic aircraft emissions were performed (Figure 4, Figure 5, and Figure 6).
- APMT-IC was tested by using the outputs of atmospheric responses to representative supersonic aircraft emissions.
- The climate, air quality, and ozone impact sensitivities developed in Task 4 by using GEOS-Chem simulations were calibrated with these estimates.

Major Accomplishments

- Three years of GEOS-Chem simulations using the supersonic emissions inventory developed by MIT and informed by the ASCENT Project 47 engine design were completed.
- The emissions inventory developed by the ASCENT 10 supersonic aircraft design team has also begun to be processed for simulation with GEOS-Chem.

Publications

None

Outreach Efforts

Progress on all tasks was communicated during biweekly briefing calls with the FAA and reported in quarterly progress reports.

Awards

None.

Student Involvement

During the reporting period of AY 2021–2022, the MIT graduate student involved in this task was Lucas Jeongsuk Oh.

Plans for Next Period

During the next project period, the project team will continue to conduct spin-up simulations and detailed analysis of the climate, air quality, and ozone impacts to supersonic aviation, on the basis of the data provided in Task 1. In addition, the team will continue calibrating the climate, air quality, and ozone impact sensitivities developed in Task 4 by using Task 3 GEOS-Chem simulations.

Task 4 - Calculation of Atmospheric Sensitivity Matrices

Massachusetts Institute of Technology

Objective

The objective of this task is to convert the impacts calculated under Task 3 for each scenario into sensitivities of environmental impacts with regard to key parameters. This process will enable the evaluation of local outcomes in air quality and support Task 5 in the rapid quantification of environmental impacts from any inventory with gridded emissions.

Research Approach

This task requires a set of GEOS-Chem simulations in which representative perturbations of a species are included over a predefined region. By calculating the change in environmental impact quantities (zonal mean ozone, surface particulate matter, and so on), the sensitivity of these quantities to emissions in each region can be determined. Linear combination of the sensitivities can then be performed to represent diverse emissions cases, including new altitude distributions, geographical distributions, and exhaust compositions for subsonic and supersonic aviation.

The team conducted sensitivity analysis for emissions at altitudes up to 26 km atmosphere, divided into a cruise (above 8 km) and non-cruise (under 8 km) region. Above 8 km, 40 regions are specified on the basis of latitude and altitude only. Below 8 km, we specify six regions on the basis of longitude and latitude. Each region (e.g., North America, Europe, and the Middle East) is defined as a compromise to ensure that areas where emissions from aviation are likely to grow differently are independently modeled while also minimizing the number of distinct regions (because each requires additional simulations to characterize). Detailed information on the non-cruise case is shown in Figure 7.

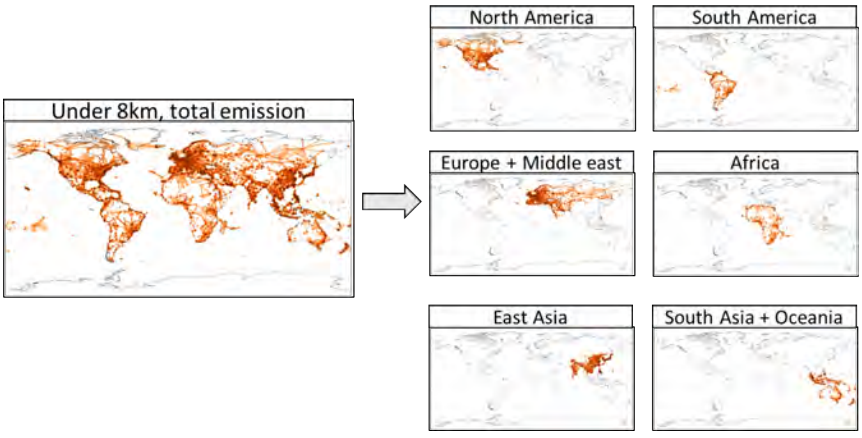

Figure 7. Illustration of the six geographical regions specified below 8 km for sensitivity analysis. The values shown in each panel are proportional to the total annual fuel burn from aviation.

Changes in model output (i.e., air quality, ozone column, RF, etc.) were taken as the sensitivity of that output to an emission anywhere within the source region. This approach is illustrated in Figure 8. By covering the full range of target altitudes, a gridded sensitivity map can be reconstructed, wherein changes in gridded outputs can be evaluated through element-wise multiplication of the sensitivities with a gridded aircraft emissions distribution (Figure 9). We have performed GEOS-Chem

simulations to quantify the climate, ozone, and air quality responses to aviation NO_x emissions for the first 5 years. Figure 10 shows these outcomes averaged over all years.

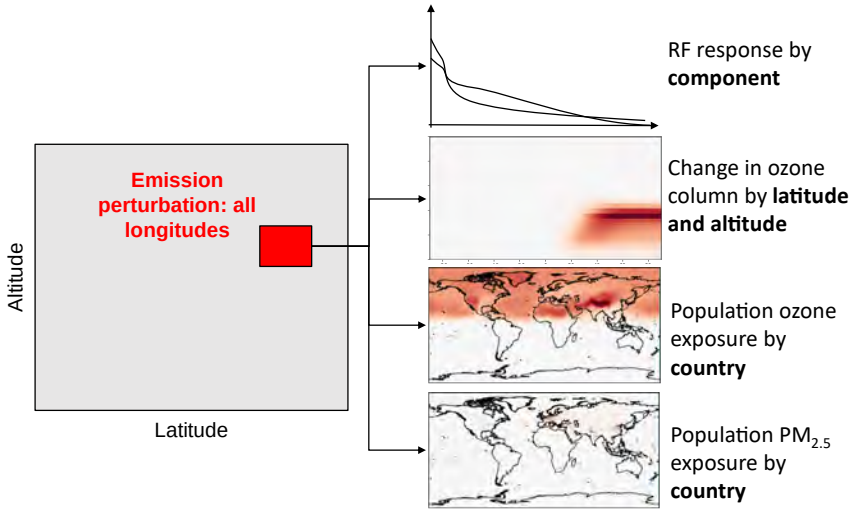

Figure 8. Approach for estimating emissions sensitivities derived from GEOS-Chem. Outputs were generated for 40 separate cruise regions and six separate non-cruise regions for 10+ years. Column ozone and air quality impacts were saved at a spatial resolution of 2˚×2.5˚. Outputs were normalized on a per-unit NO_x emissions basis.

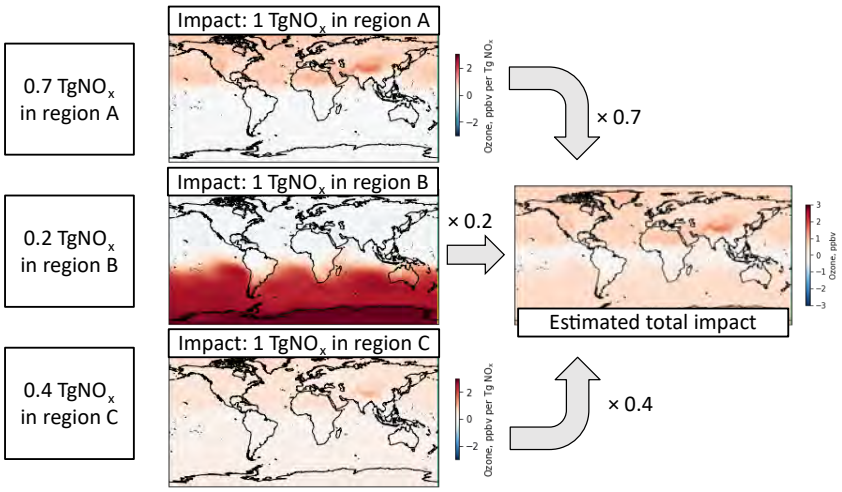

Figure 9. Example case analysis using linearized NO_x emissions sensitivities. Environmental impacts were estimated as the weighted sum of each sensitivity region's impacts, wherein the weights are the amount of NO_x in each region.

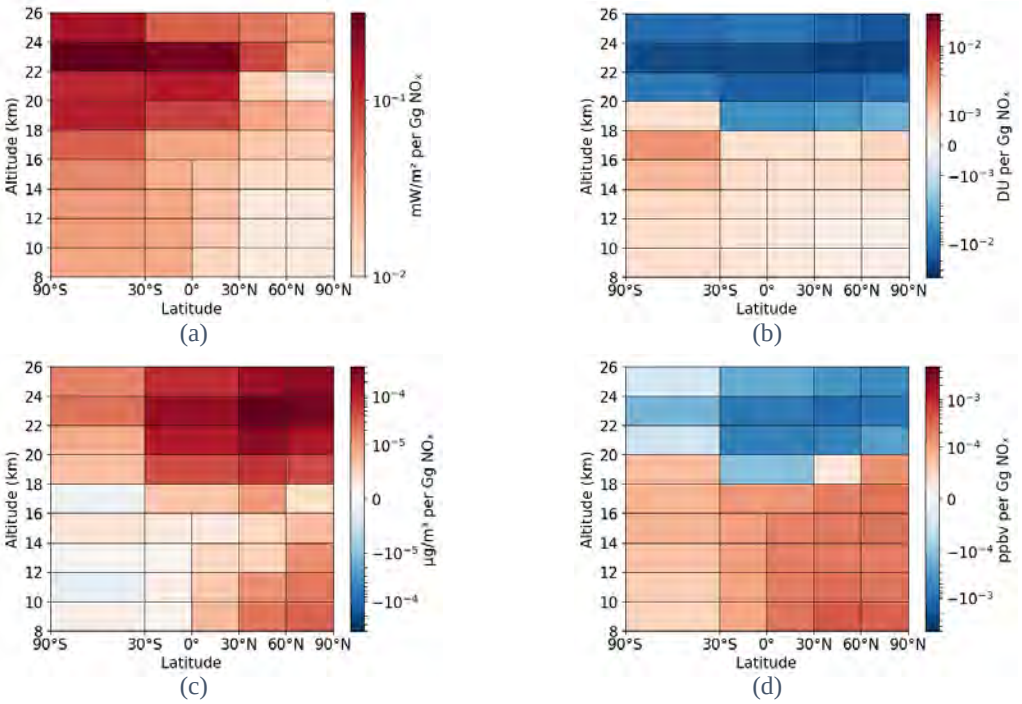

Figure 10. Spatially discretized NO_x sensitivity results averaged over the first 5 years for cruise regions: (a) radiative forcing (RF), (b) global average column O_3, (c) population-weighted average $PM_{2.5}$ exposure, and (d) population-weighted average surface O_3 exposure. The sensitivities at cruise altitudes are defined by altitude and latitude dimensions. Averaged column O_3, $PM_{2.5}$ exposure, and surface O_3 exposure impacts can be expanded into local (gridded) results.

The basic procedure for estimating total impact from a given emissions scenario is shown in Figure 9. We currently assume that the relationship between emissions and impacts is approximately linear, although this assumption may be revised for very large emission rates, on the basis of further analysis.

To test this assumption, we performed an analysis that aggressively tests the linearity assumption. Figure 11 shows how ozone in a single cell responds to increased emissions of ozone in a single region. The red line shows the estimated linear slope to be used in APMT-IC, whereas the black line shows the "true" results. We found that the linear fit performs well for emissions rates below 200 Gg NO_x/year, although deviations from the linear case were observed for very high emissions rates (above 300 Gg NO_x/year). As a reference, for ASCENT 10, the maximum NO_x emitted in each region corresponds to 360 Gg and 106 Gg for the MIT High case. Thus, the existing procedure is sufficient for evaluation of supersonic aviation up to the scale predicted by the MIT High case, but an additional set of simulations may be needed to capture the behavior of very high-uptake scenarios such as the ASCENT 10 prediction.

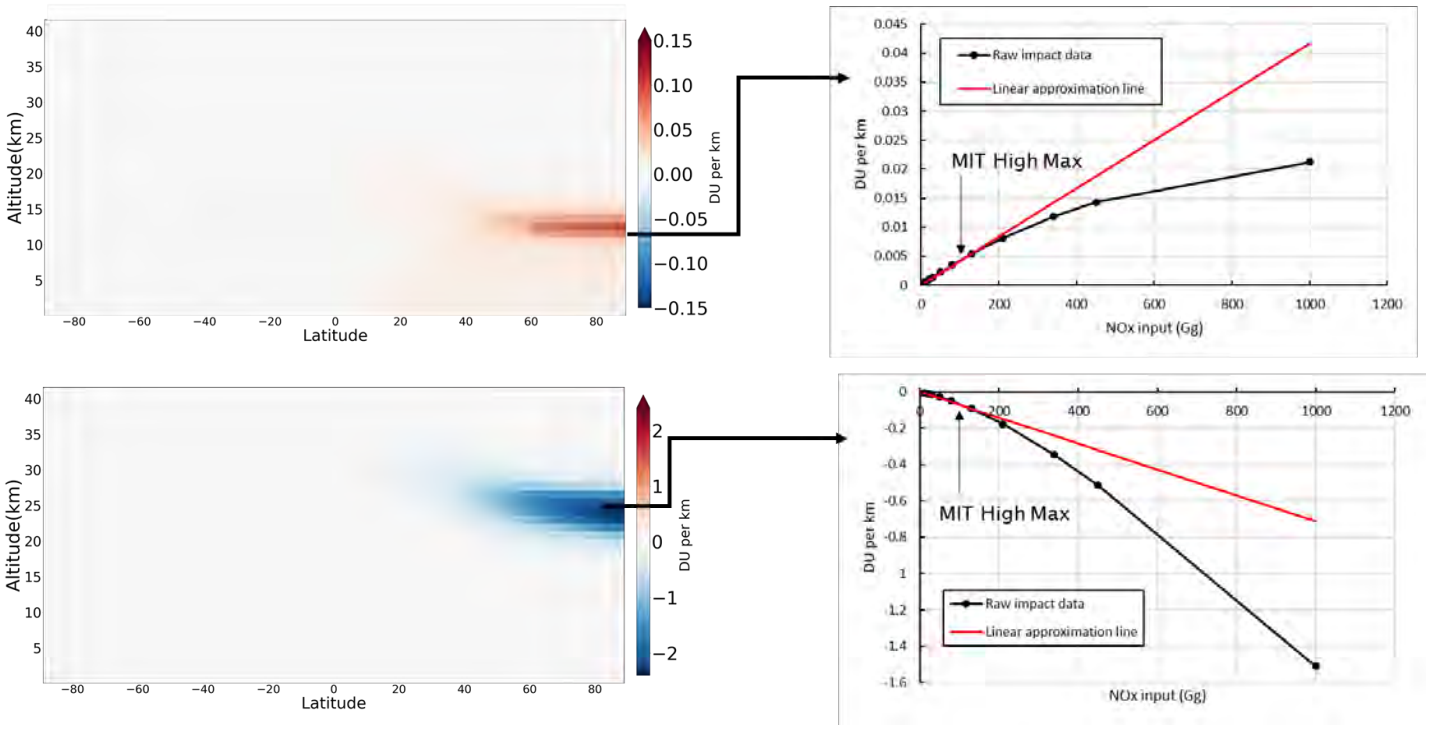

Figure 11. Response of the zonal ozone according to the amount of NO_x. Left: example cases for checking linearity (left column); right: results with linear estimation (right column).

Ultimately, our team evaluated the consistency between the sensitivity-based approach and GEOS-Chem forward model by calculating impacts for using the MIT High case from Task 1 with both methods (Figure 12 through Figure 14). Although analysis is ongoing, the results have shown good qualitative agreement to date and have been implemented in the upgraded APMT under Task 5.

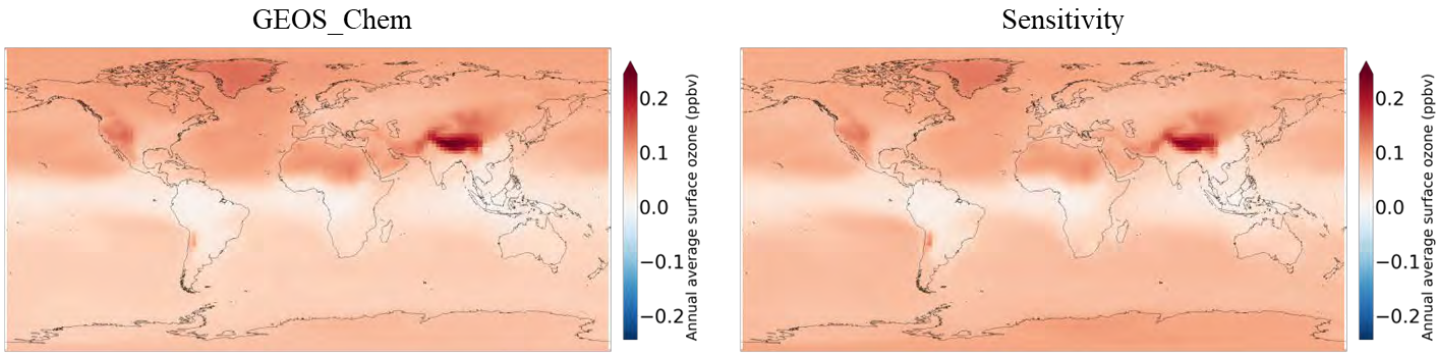

Figure 12. MIT High case third year D (test case − baseline) map for annual average surface ozone for GEOS-Chem (left) and sensitivity (right) cases; ppbv = parts per billion per volume.

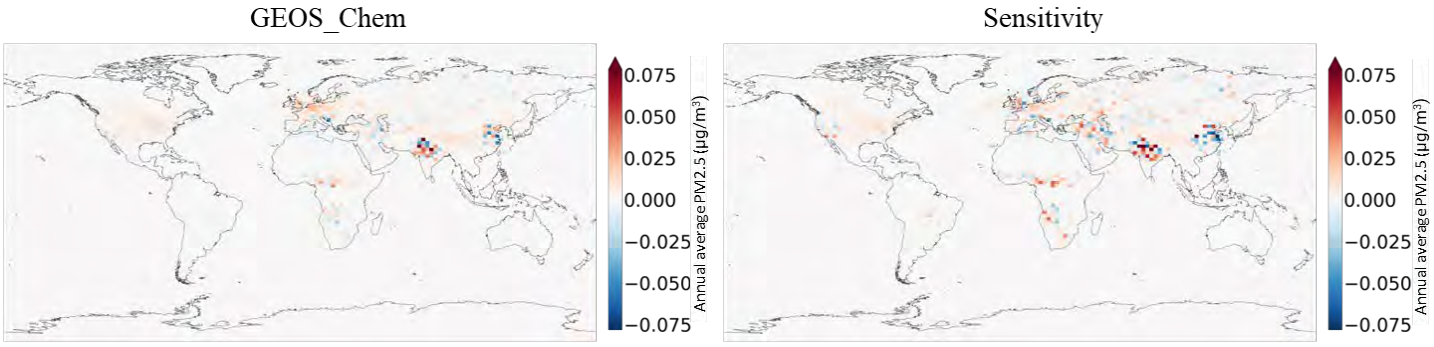

Figure 13. MIT High case third year D (SST scenarios − baseline) map for $PM_{2.5}$ for GEOS-Chem (left) and sensitivity (right) cases; mg/m^3 = micrograms per cubic meter.

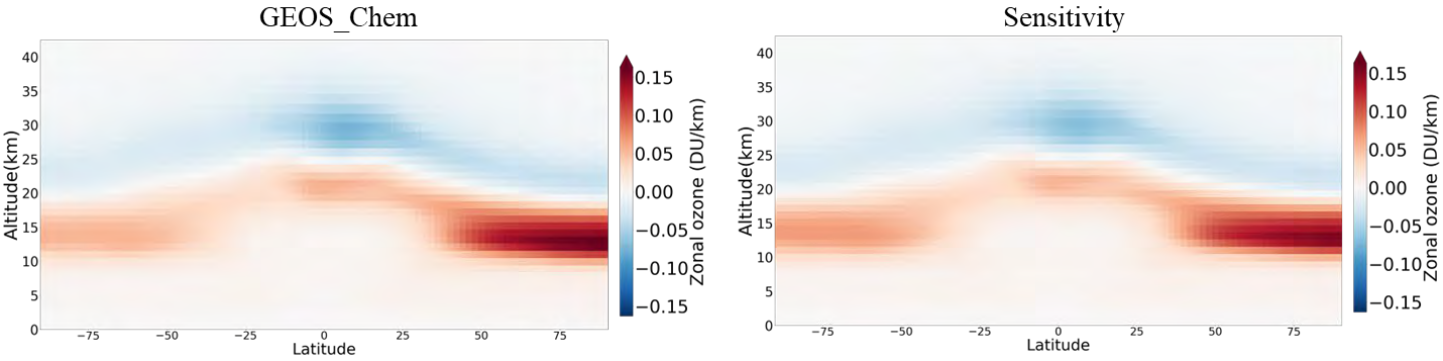

Figure 14. MIT High case third year D (SST scenarios − baseline) map for zonal ozone for GEOS-Chem (left) and sensitivity (right) cases; DU/km = Dobson units per kilometer.

Milestones

- A refined discretization of the atmosphere to distinguish between non-cruise and cruise altitudes has been established.
- Simulations in GEOS-Chem to evaluate the atmospheric responses to representative perturbations in each region for NO_x emissions have been obtained for 5 years, thus enabling an initial assessment of the accuracy of the sensitivity-based approach.

Major Accomplishments

- Estimates of impacts for the MIT SST and ASCENT 10 emissions inventories have been compared by using the linearized NO_x emissions sensitivities and full GEOS-Chem forward simulations.
- Communication with the ASCENT 22 team has begun for qualitative model intercomparison regarding the environmental impacts of supersonic aircraft emissions.

Publications

None.

Outreach Efforts

Progress on all tasks was communicated during biweekly briefing calls with the FAA and reported in quarterly progress reports.

Awards
None.

Student Involvement
For the AY 2021–2022 reporting period, graduate students Lucas Jeongsuk Oh and Joonhee Kim were involved with this task.

Plans for Next Period
During the next project period, the project team will generate gridded sensitivity data for as many as 10 years of NO_x emissions, as well as sensitivity data for H_2O, black carbon, and SO_x. Where necessary, additional simulations will be performed to refine the regions for which sensitivities are calculated. A limited set of additional "extreme case" simulations may also be performed to understand the degree of non-linearity in the response of ozone to NO_x.

Task 5 - Develop and Update Operational Tools Capable of Quantifying Environmental Impacts of Aviation
Massachusetts Institute of Technology

Objective
The objective of this task is to operationalize the results of Tasks 1–4. The eventual outcome will be a re-engineered version of APMT for climate and air quality impacts, calibrated on the basis of updated sensitivity data, and upgraded to provide monetized impacts that consider the possibility of different cruise altitudes (among other characteristics). Ozone layer impacts will also be provided in the updated model.

Research Approach
This task aims to produce a more broadly capable operational tool by reimplementing the APMT-IC structure in the Julia programming language. During AY 2021–2022, the most recent GEOS-Chem sensitivity data for NO_x emissions described in Task 4 were implemented in the updated (in development) APMT, along with the framework for other key emission species. The team also updated APMT to incorporate current scientific understanding of climate modeling from the Intergovernmental Panel on Climate Change (IPCC) Sixth Assessment Report (AR6). The high-level model overview is shown in Figure 15.

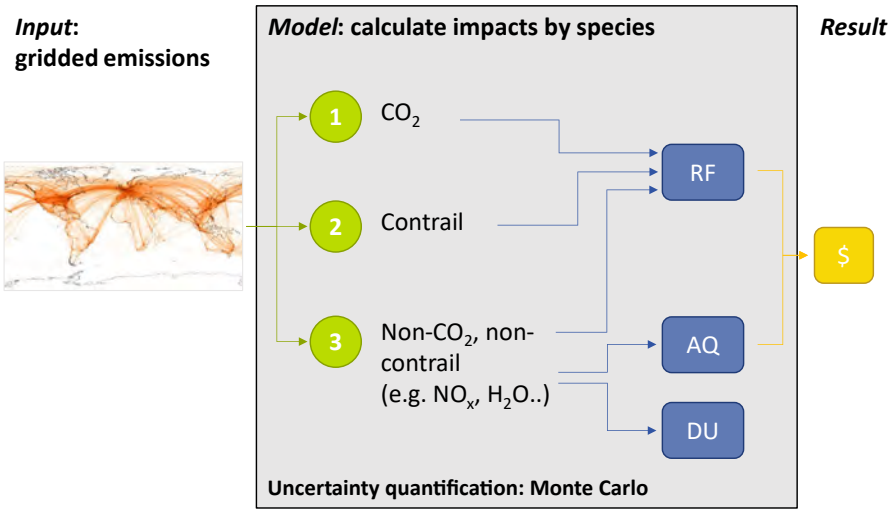

Figure 15. Model overview.

In APMT, impacts are calculated for the following groups of species: (a) CO_2, (b) contrails, and (c) non-CO_2, non-contrail, as described in detail below.

1. CO_2 is a well-mixed greenhouse gas whose impacts are insensitive to the location of emissions. Its climate sensitivities have been updated to correspond to the background CO_2 concentrations, according to the Shared

Socioeconomic Pathways (SSPs). The team calculated Impulse Response Functions (IRFs) (Joos et al., 2013) by running the Model for the Assessment of Greenhouse Gas Induced Climate Change (MAGICC6) (Meinhausen et al., 2011), as shown in Figure 16. IRFs represent the time-dependent abundance of CO_2 caused by an additional unit of emissions at the time of emission.

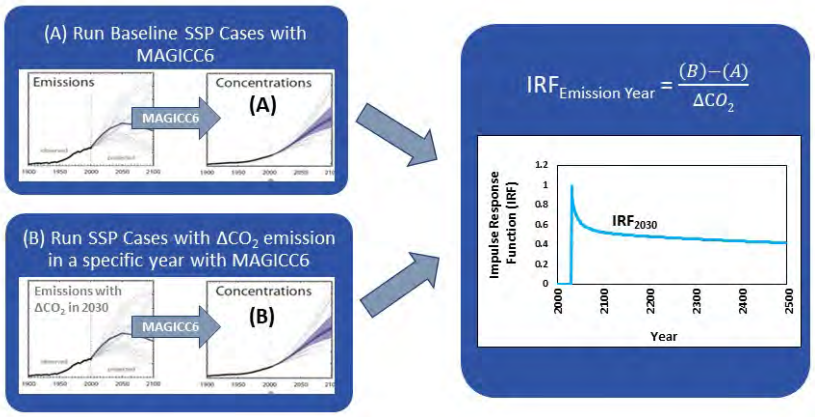

Figure 16. Schematic describing the method used to calculate CO_2 IRFs.

Figure 17 shows the IRFs for four SSP scenarios. The data in red represent MAGICC6 outputs, and the data in gray represent extrapolated data. The RF calculation for a given CO_2 concentration has also been updated to include interactions between CO_2 and N_2O, according to the most recent spectroscopic data (Etminan et al., 2016).

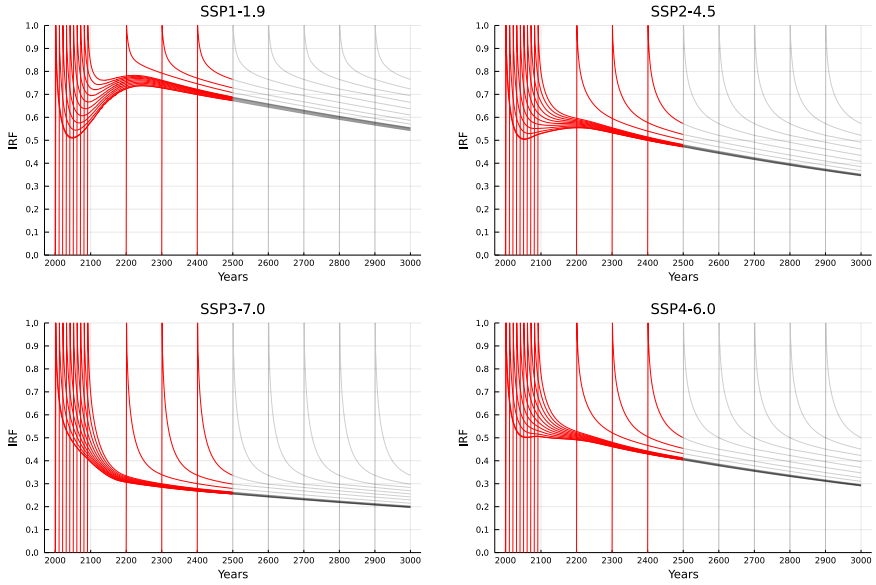

Figure 17. Updated IRFs for scenarios SSP1-1.9, SSP2-4.5, SSP3-7.0, and SSP4-6.0. The first number of the scenario labels refers to the SSP (1–5), and the second number refers to approximate global effective RF in 2100. These emissions scenarios supersede the representative concentration pathways used in previous versions of APMT-IC.

2. The climate impacts of contrails have been updated to incorporate the differential contrail forcing by region, as described in Task 6.

3. Finally, the framework for non-CO_2, non-contrail (e.g., NO_x, SO_x, black carbon, and H_2O) emissions sensitivities has been included. During AY 2021–2022, NO_x sensitivities were implemented to estimate the climate, air quality, and ozone column impacts. As described in Task 4, these sensitivities regionalize the air quality impacts to show outcomes by country for exposure to fine particulate matter ($PM_{2.5}$) and surface ozone.

In APMT, climate RF impacts are translated into temperature change and resulting damages. The background temperature change was also calibrated to updated SSP emission backgrounds by using MAGICC6 for an appropriate range of equilibrium climate sensitivity values. Figure 18 shows the distribution of the background temperature change relative to the 1850–1900 IPCC reference period for several SSP scenarios.

Health impact calculations were extended to include the Global Exposure Mortality Model concentration response function from Burnett et al. (2018) for population $PM_{2.5}$ exposure. Future projections of country-level population and gross domestic product have also been updated to correspond to the SSP scenarios.

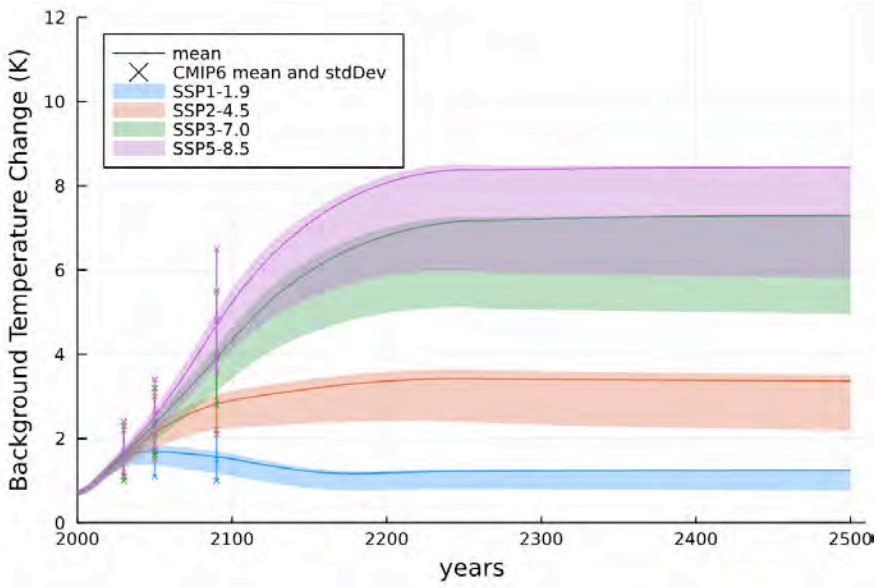

Figure 18. Updated SSP background temperature change. The shaded regions indicate percentiles 33–67, and the solid lines indicate the mean temperature change. The skewed distribution is driven by the Roe and Baker (2007) distribution used by U.S. federal agencies from the most recent social cost of carbon estimates. The CMIP6 temperature estimates (mean and 90% CI) reported in AR6 are also shown for comparison.

Milestones

- The team presented a preliminary demonstration to the FAA on how to run the updated APMT, including specifying the inputs of gridded aviation emissions and interpreting the climate and air quality impact results.
- Data for CO_2 concentrations, background temperature change, country-level gross domestic product growth, and population projections have been updated on the basis of SSP scenarios.
- The framework for emissions sensitivity has been incorporated into the model, as well as the first 5 years of NO_x sensitivity data from Task 4.

Major Accomplishments

- APMT is now capable of estimating localized air quality and column ozone impacts.
- Health impacts can be calculated in APMT by country and for multiple concentration response functions.
- AMPT also includes impact trajectories corresponding to the most recent SSP scenarios from IPCC AR6, thus ensuring policy relevance.

Publications
None.

Outreach Efforts
Progress on all tasks was communicated during biweekly briefing calls with the FAA and reported in quarterly progress reports. A poster presentation was provided on the updates to APMT and the trade-offs associated with high-altitude NO_x emissions at the Fifth International Conference on Transport, Atmosphere and Climate, 2022 (TAC-5). In addition, the previous version of APMT was used to derive climate impacts for a study focusing on identifying aviation cost and emissions pathways toward net-zero climate impacts by 2050 (Dray et al., 2022).

Awards
None.

Student Involvement
During the reporting period of AY 2021–2022, the MIT graduate student involved in this task was Joonhee Kim.

Plans for Next Period
The project team will integrate the larger set of Task 4 sensitivities into the new version of APMT, including future years for NO_x as well as other key emission species. APMT will then be used to evaluate the monetized climate and air quality damages for multiple subsonic or SST inventories. The tool will also include accessible output and visualization of outcomes.

References
Burnett, R., Chen, H., Szyszkowicz, M., Fann, N., Hubbell, B., Pope, C. A., Apte, J. S., Brauer, M., Cohen, A., Weichenthal, S., Coggins, J., Di, Q., Brunekreef, B., Frostad, J., Lim, S. S., Kan, H., Walker, K. D., Thurston, G. D., Hayes, R. B., … Spadaro, J. V. (2018). Global estimates of mortality associated with long-term exposure to outdoor fine particulate matter. *Proceedings of the National Academy of Sciences*, *115*(38), 9592–9597. Doi: 10.1073/pnas.1803222115

Dray, L., Schäfer, A. W., Grobler, C., Falter, C., Allroggen, F., Stettler, M. E. J., & Barrett, S. R. H. (2022). Cost and emissions pathways towards net-zero climate impacts in aviation. *Nature Climate Change*, *12*(10), 956–962. Doi: 10.1038/s41558-022-01485-4

Etminan, M., Myhre, G., Highwood, E. J., & Shine, K. P. (2016). Radiative forcing of carbon dioxide, methane, and nitrous oxide: A significant revision of the methane radiative forcing. *Geophysical Research Letters*, *43*(24). Doi: 10.1002/2016GL071930

Joos, F., Roth, R., Fuglestvedt, J. S., Peters, G. P., Enting, I. G., von Bloh, W., Brovkin, V., Burke, E. J., Eby, M., Edwards, N. R., Friedrich, T., Frölicher, T. L., Halloran, P. R., Holden, P. B., Jones, C., Kleinen, T., Mackenzie, F. T., Matsumoto, K., Meinshausen, M., … Weaver, A. J. (2013). Carbon dioxide and climate impulse response functions for the computation of greenhouse gas metrics: A multi-model analysis. *Atmospheric Chemistry and Physics*, *13*(5), 2793–2825. Doi: 10.5194/acp-13-2793-2013

Meinshausen, M., Raper, S. C. B., & Wigley, T. M. L. (2011). Emulating coupled atmosphere-ocean and carbon cycle models with a simpler model, MAGICC6 – Part 1: Model description and calibration. *Atmospheric Chemistry and Physics*, *11*(4), 1417–1456. Doi: 10.5194/acp-11-1417-2011

Roe, G. H., & Baker, M. B. (2007). Why is climate sensitivity so unpredictable? *Science*, *318*(5850), 629–632. Doi: 10.1126/science.1144735

Task 6 - Regionalized Parameterization of Contrails
Massachusetts Institute of Technology

Objective
This task aims to parameterize contrails, linking distance flown in a given region to the expected RF. In the existing version of APMT-IC (v24c), the total impacts of emissions are quantified per unit of additional fuel burned for the current subsonic fleet. A review by Lee et al. (2020) of aviation's impacts from 2000 to 2018 has highlighted two specific gaps in the APMT-IC framework for estimating contrail RF impacts. The first gap is the need for a more sophisticated representation of the contrail impacts from the number and distribution of flights. Owing to the complex relationship between contrail production and other engine parameters, estimating contrail impacts per unit of distance flown is a better metric than per unit of fuel burn. The second gap is that the brief, localized nature of contrails, as well as the sensitivity of contrail production to

surrounding weather conditions, leads to probable differences in the likelihood of contrail formation as a function of location. Therefore, the objective of this task is to link the distance flown in a given region to the expected RF.

Research Approach

Parameterization of contrail formation on the basis of only the quantity of fuel burned, or even total global cruise flight distance, does not consider the localized nature of the likelihood of contrail formation as a function of region or the climate impact resulting from a persistent contrail. To address these gaps, the new framework of APMT incorporates the spatial distribution of contrail RF impacts per flight distance flown from Agarwal (2021).

Figure 19 shows the distribution of the mean contrail energy forcing per distance flown in specific region for cruise altitudes between 9 and 12 km. The regions are defined as North America, contiguous United States, Western Europe, Russia, Middle East, South and East Asia, North Atlantic, South Atlantic, North Pacific, Central Pacific, and all remaining areas.

These regional distributions were obtained in Agarwal (2021) by using the central limit theorem with a sufficiently large number of samples. The mean value of the random samples in each region is normally distributed, and confidence intervals with 95% likelihood of containing the sample mean were provided. The confidence intervals representing the uncertainty from using a sampling-based approach to estimate contrail RF impacts were included in APMT. To account for the uncertainty due to uncertain contrail properties, APMT aligns with the overall contrail RF uncertainty of ±70% in Lee et al. (2020).

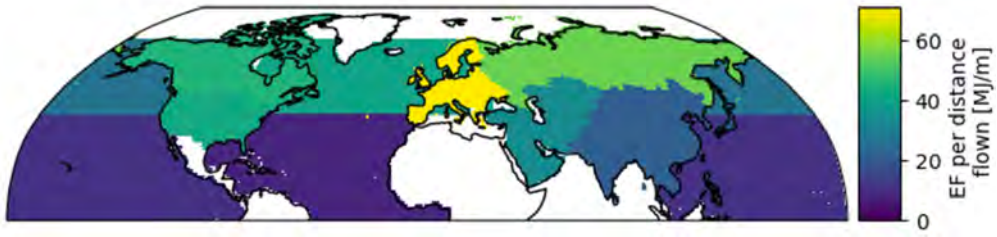

Figure 19. Spatial distribution of mean contrail energy forcing (EF) per distance flown in the Northern Hemisphere (Agarwal 2021).

Contrail impacts provided as the energy forcing (EF) per distance flown were obtained from an annual flight schedule. They were converted in APMT to the RF per distance flown by dividing the EF by the Earth's surface area and the number of seconds in a year.

$$\text{RF per distance flown} = \frac{\text{EF per distance flown}}{\text{surface area} \cdot \text{seconds per year}} = \frac{\text{J}}{\text{m flown}} \cdot \frac{1}{\text{m}^2 \cdot \text{sec}} = \frac{\text{W} \cdot \text{sec}}{\text{m flown}} \cdot \frac{1}{\text{m}^2 \cdot \text{sec}} = \frac{\text{W/m}^2}{\text{m flown}}$$

The code being developed in Julia for APMT now accepts gridded flight distances. The total contrail RF impact for a given emissions inventory was calculated as the linear sum of each region's RF per distance flown multiplied by the distance flown in that region (r_c).

$$\text{RF}_{\text{contrail}} = \sum_{r_c} (\text{RF}_{\text{contrail}} \text{ per flight km})_{r_c} \times (\text{flight km})_{r_c}$$

In IPCC's AR6, effective RF (ERF) was recommended to be used as a more useful measure of the global temperature response than the RF metric. To adjust the estimated RFs from Agarwal (2021) to ERFs, the model applies the ERF/RF ratio derived from Bickel et al. (2020), Ponater et al. (2006), and Rap et al. (2010). This ratio is modeled as an uncertain variable with a triangular distribution with a minimum value of 0.31, mode of 0.42, and maximum of 0.59 (fraction).

Milestones

- APMT has been updated to accept gridded flight distances.
- Coarsely defined regions and the expected average contrail forcing resulting from 1 km of flight in those regions, on the basis of Agarwal (2021), have been included in the model.

Major Accomplishments
The team has implemented the contrail "RF by location" sensitivities, thus resulting in the first reduced-order, flexible tool for rapid evaluation of aviation's contrail-related climate impacts.

Publications
None.

Outreach Efforts
Progress on all tasks was communicated during biweekly briefing calls with the FAA and reported in quarterly progress reports.

Awards
None.

Student Involvement
During the reporting period of AY 2021–2022, the MIT graduate student involved in this task was Joonhee Kim.

Plans for Next Period
Task 6 was largely completed in AY 2021–2022. During the next reporting period, the team plans to evaluate the altitude sensitivity of contrail impacts. The model currently does not estimate regional contrail RF for high-altitude aviation.

References
Agarwal, A. (2021). *Quantifying and reducing the uncertainties in global contrail radiative forcing* [Doctoral thesis, Massachusetts Institute of Technology]. https://dspace.mit.edu/bitstream/handle/1721.1/140372/agarwal_aa681_PhD_AeroAstro_thesis.pdf?sequence=1&isAllowed=y

Bickel, M., Ponater, M., Bock, L., Burkhardt, U., & Reineke, S. (2020). Estimating the effective radiative forcing of contrail cirrus. *Journal of Climate*, *33*(5), 1991–2005. Doi: 10.1175/JCLI-D-19-0467.1

Lee, D. S., Fahey, D. W., Skowron, A., Allen, M. R., Burkhardt, U., Chen, Q., Doherty, S. J., Freeman, S., Forster, P. M., Fuglestvedt, J., Gettelman, A., De León, R. R., Lim, L. L., Lund, M. T., Millar, R. J., Owen, B., Penner, J. E., Pitari, G., Prather, M. J., Sausen, R., & Wilcox, L. J. (2020). The contribution of global aviation to anthropogenic climate forcing for 2000 to 2018. Atmospheric Environment, 117834. Doi: 10.1016/j.atmosenv.2020.117834

Ponater, M., Pechtl, S., Sausen, R., Schumann, U., & Hüttig, G. (2006). Potential of the cryoplane technology to reduce aircraft climate impact: A state-of-the-art assessment. *Atmospheric Environment*, *40*(36), 6928–6944. Doi: 10.1016/j.atmosenv.2006.06.036

Rap, A., Forster, P. M., Haywood, J. M., Jones, A., & Boucher, O. (2010). Estimating the climate impact of linear contrails using the uk met office climate model: Climate impact of linear contrails. *Geophysical Research Letters*, *37*(20). Doi: 10.1029/2010GL045161

Task 7 - Investigate the Dependence of Aviation Emissions Impacts on Non-Aviation Factors
Massachusetts Institute of Technology

Objective
Aviation emissions since the start of the jet age have caused present-day climate impacts through CO_2 and non-CO_2 impacts (Grobler et al., 2019; Lee et al., 2020) and have also been responsible for air quality impacts over this time. These atmospheric impacts have been shown to vary by the region of emissions, emissions altitude, and season of emissions (Fichter et al., 2005; Gilmore et al., 2013). Additionally, contrail climate impacts are sensitive to particle number emissions (Bock and Burkhardt, 2016; Teoh et al 2019). The non-CO_2 climate impacts continue to propagate over years to decades through their impact on global surface temperature.

Over the past 40 years, the region, altitude, and chemical composition of aviation emissions have varied. Therefore, evaluation of present-day and future impacts from aviation requires accurate estimate of aviation's emissions over the past 40 years. Existing aviation impact assessments have relied on evaluation of specific years, and/or have scaled these impacts

by fuel and emissions, which do not capture heterogeneities in the region and altitude of emission (Lee et al., 2020). Consequently, the total cumulative temperature change and the air quality impacts attributable to aviation remain uncertain.

The objective of this task is to understand how the impacts of aviation have been driven by changes in both aviation and non-aviation factors. We first will derive a bottom-up emissions inventory for global commercial civil aviation spanning the jet age from 1980 to present day in 2019. This inventory will be the first to capture differences in region, altitude, and chemical composition of the emissions over this time span.

The results will provide insights into trends in emissions over time, such as emissions quantities by species, location, and season. As such, we will obtain insights into how changes in fleet composition as well as aircraft and engine design have changed the importance of pathways through which aviation influences the climate. Furthermore, this work will enable a future assessment of how these changes in emissions characteristics have affected the cumulative climate impact of aviation.

The second component of this research is to use atmospheric modeling to investigate the influence of both changes in aviation emissions and changes in non-aviation factors regarding environmental outcomes. This component includes both an investigation of the effects of the historical emissions described above, and an investigation of the mechanisms underlying aviation's ongoing impacts.

Research Approach

Global aviation operation data were obtained from Official Airline Guide schedule data. For 1980–2010, these data are at 5-year resolution; for 2013–2019, these data are at 1-year resolution. Aircraft performance and fuel burn were quantified with Base of Aircraft Data 3 (BADA3). Emissions species of NO_x, HC, and CO were determined from the ICAO Emissions Databank. These ground-level emissions from the ICAO Emissions Databank were extended to cruise altitude by using Boeing Fuel Flow Method 2. Non-volatile particulate mass and particle number emissions were estimated by using the SCOPE11 correlation method and, if available, direct measurements (Agarwal et al., 2019; Ahrens et al., 2022).

The preliminary derived fuel burn totals were compared with fuel burn totals from other studies in the literature, as shown in Figure 20. This figure includes the International Energy Agency (aviation fuel burn totals. This statistic represents the total annual fuel consumption of fuels meeting jet fuel specifications and may include fuel that is used in other applications, such as ground vehicles, engine testing and other uses (Olsen et al., 2013). As such, these International Energy Agency totals are considered a theoretical upper bound of aviation jet fuel usage (Olsen et al., 2013). Other aviation emissions inventories are also plotted in Figure 20, with our preliminary annual fuel burn totals matching studies with a similar scope.

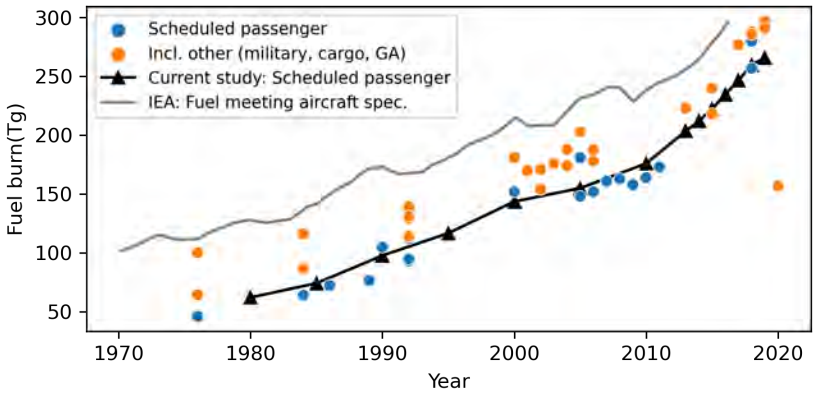

Figure 20. Comparison of our preliminary annual fuel burn totals with fuel burn totals in the literature.

These fuel burn totals were gridded into the locations where the emissions occur (Figure 21 and Figure 22). In 1980, the largest contribution of fuel burn was from North America, and by 2019 North America, Europe, and East Asia had similar contributions to total global annual fuel burn. Over this period, the emissions share in North America is halved, whereas the share in East Asia is tripled. This change in regional distribution is likely to affect the magnitude of climate and air quality impacts over time, because emissions in different regions lead to different climate impacts, sometimes differing by more than a factor 2 (Lund et al., 2017).

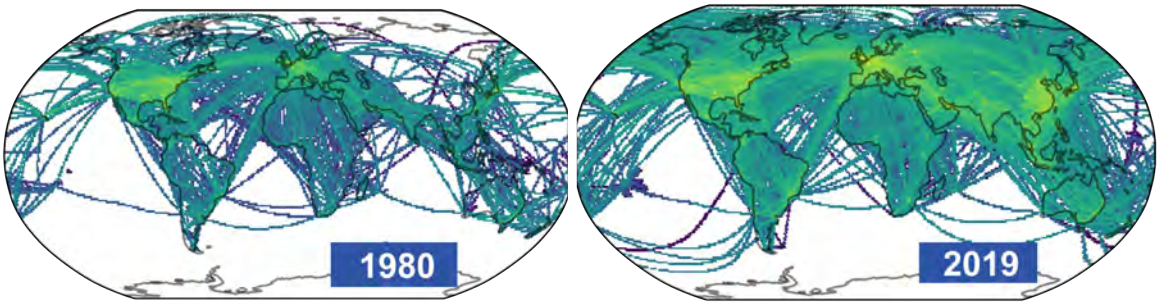

Figure 21. Preliminary locations of emissions in 1980 (left) and 2019 (right).

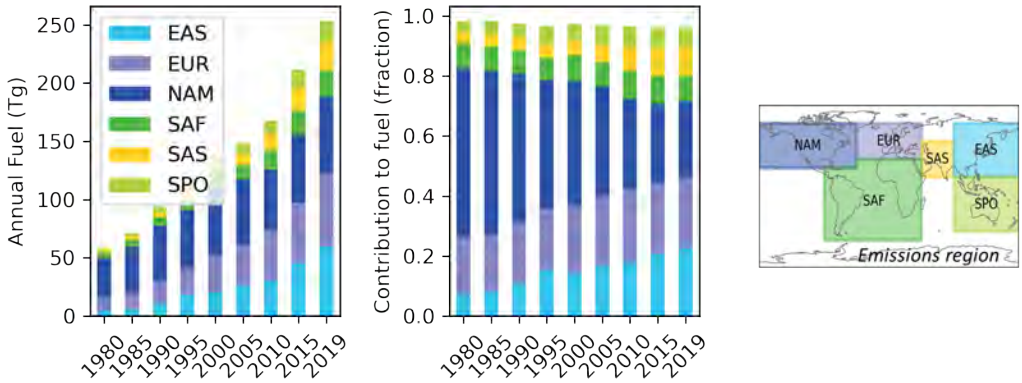

Figure 22. Evolution of regions of aviation emissions over time. Emissions outside the six indicated areas are negligible; totals can be inferred as the difference between the totals in the center lower panel and 1.0.

We also investigated the differences in the times of day when emissions occur. This aspect is important, because contrail lifetimes are typically only several hours, and their radiative impacts are sensitive to the time of day when contrails occur and persist. We consider four regions (United States, North Atlantic, Europe and Asia), and plot the fraction of fuel burn occurring in each region by the hour of the day (Figure 23). The figure also shows the local daytime/nighttime at the center of the region. In all four regions, our preliminary results indicated that the share of fuel burn occurring during the night increases, thus indicating a potential increase in contrail impacts per unit fuel burn over this period.

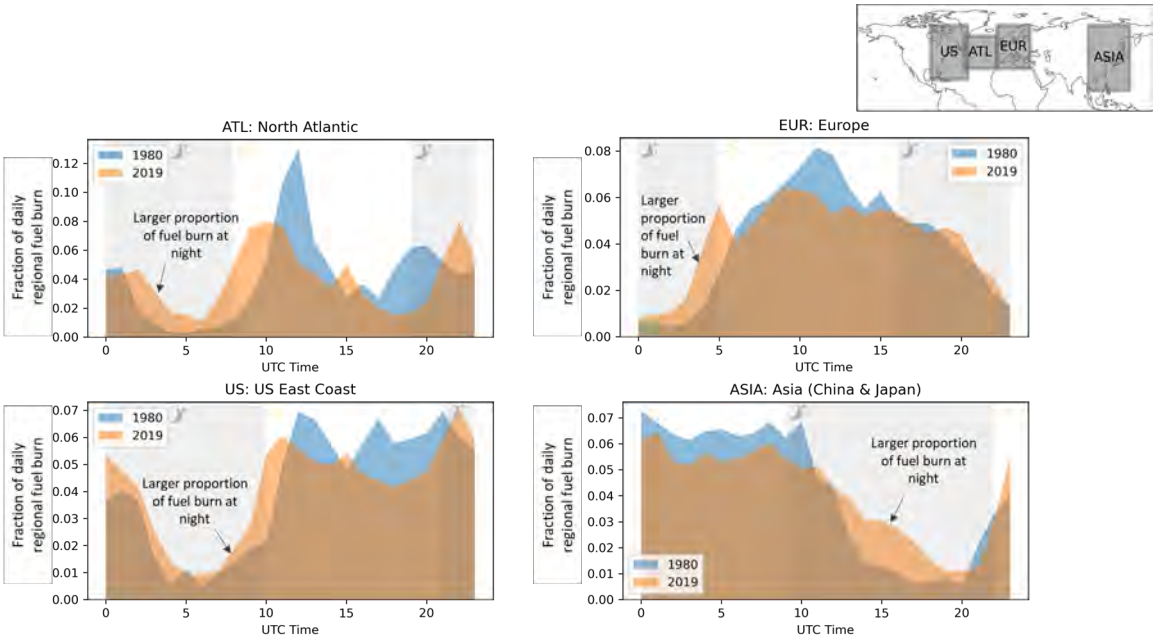

Figure 23. Difference in fuel burn by time of day between 1980 and 2019. In all regions considered, the fraction of fuel burn occurring during the night increases.

The final trend investigated involves how the emissions composition of NO_x and nonvolatile particulate matter (nvPM) changes over time. Our preliminary results showed that NO_x emissions increased by 36% over this period, and nvPM emissions decreased by 76% (Figure 24). Figure 24 also shows the distribution of emissions indices of the different engines that make up the total fleet-wide NO_x and nvPM emissions indices, thus indicating a variation among different engines of more than an order of magnitude. Therefore, these results may be sensitive to the specific aircraft-engine matchings selected in the emissions software. Consequently, further work is needed to further refine these aircraft–engine matchings in the emissions software.

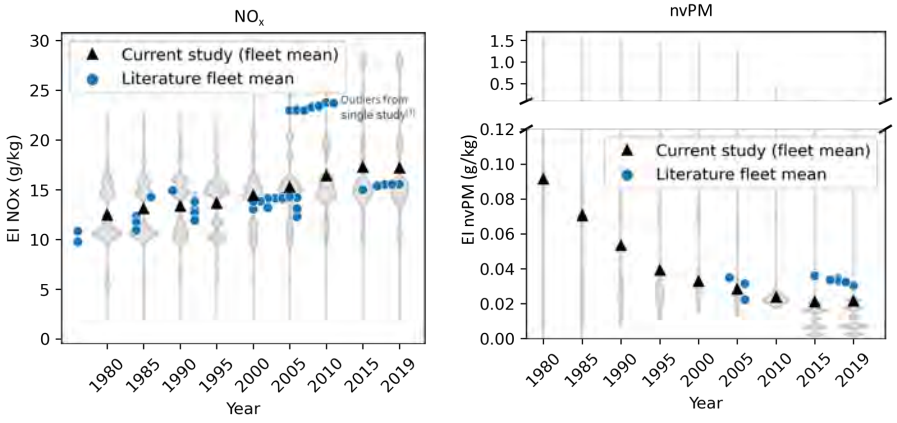

Figure 24. For NO_x, the outliers are all from the same study (Waisuik et al 2016). Note: these results are only preliminary.

Most of our investigation of the mechanisms underlying aviation's impacts, and its relationships with aviation and non-aviation factors, will be performed by using the data derived from the above work. However, we have also started performing parallel simulations to tease apart how aviation emissions alter atmospheric composition, including the role of aviation NO_x and SO_x in changing global aerosol burdens and their climate impacts. A manuscript on this work was presented at the TAC-

5 conference and published this year (Prashanth et al., 2022). By separately investigating each emissions component in simulations with the GEOS-Chem chemistry transport model, we established that aviation NO_x rather than SO_x is responsible for 72% of surface-level aerosol, but that both aviation and non-aviation SO_x significantly contribute to the overall climate impacts of aviation-attributable aerosol. This aspect is critical for understanding how different aviation emissions regulations might influence aviation's long-term environmental impacts.

Milestones

- A preliminary emissions inventory was derived by using a preliminary set of emissions schedule data.
- These emissions were compared with other inventories, and trends were investigated, including region of emissions, time of day when emissions occur, and emissions composition over time.

Major Accomplishments

A preliminary emissions inventory was derived, and trends were investigated, showing that climate and air quality impacts are likely to have varied over time. Furthermore, a manuscript was published on aviation's contribution to aerosol concentrations and the relative role of non-aviation emissions. Both sets of work were presented at an international conference in Germany in June 2022.

Publications

Grobler, C., Fritz, T., Allroggen, F., Eastham S., & Barrett, S.R. (2022). *Commercial civil aviation emissions from 1980 to the present day* [Oral presentation]. 5th International Conference on Transport, Atmosphere, and Climate (TAC-5.

Prashanth, P., Eastham, S. D., Speth, R. L., & Barrett, S. R. H. (2022). *Aerosol formation pathways from aviation emissions* [Oral presentation]. 5th International Conference on Transport, Atmosphere, and Climate (TAC-5).

Prashanth, P., Eastham, S. D., Speth, R. L., & Barrett, S. R. H. (2022). Aerosol formation pathways from aviation emissions. *Environmental Research Communications*, *4*(2), 021002. https://doi.org/10.1088/2515-7620/ac5229

Outreach Efforts

Progress on all tasks was communicated during biweekly briefing calls with the FAA and reported in quarterly progress reports. This work was also presented to the scientific community at TAC-5, in Germany, in June 2022.

Awards

None.

Student Involvement

This emissions inventory work was performed by PhD student Carla Grobler. She also presented the preliminary emissions inventory work at the TAC-5 conference in Germany. The investigation of aerosol impacts from aviation emissions was performed by Prakash Prashanth, who was also a PhD student at the time.

Plans for Next Period

During the next reporting period, the team plans to finalize the emissions inventory as follows:

- Enhance cruise altitude accuracy
- Update emissions code to use the more recent BADA 3.16 data
- Improve aircraft engine matching by using purchased fleet data or other manual methods
- Generate final gridded emissions inventory for the schedule years

References

Agarwal, A., Speth, R. L., Fritz, T. M., Jacob, S. D., Rindlisbacher, T., Iovinelli, R., Owen, B., Miake-Lye, R. C., Sabnis, J. S., & Barrett, S. R. H. (2019). Scope11 method for estimating aircraft black carbon mass and particle number emissions. *Environmental Science & Technology*, *53*(3), 1364–1373. https://doi.org/10.1021/acs.est.8b04060

Ahrens, D., Méry, Y., Guénard, A., & Miake-Lye, R. C. (2022). A new approach to estimate particulate matter emissions from ground certification data: The nvpm mission emissions estimation methodology(Meem). *Volume 3A: Combustion, Fuels, and Emissions*, V03AT04A035. https://doi.org/10.1115/GT2022-81277

Bock, L., & Burkhardt, U. (2016). Reassessing properties and radiative forcing of contrail cirrus using a climate model. *Journal of Geophysical Research: Atmospheres*, *121*(16), 9717–9736. https://doi.org/10.1002/2016JD025112

Fichter, C., Marquart, S., Sausen, R., & Lee, D. S. (2005). The impact of cruise altitude on contrails and related radiative forcing. *Meteorologische Zeitschrift*, *14*(4), 563–572. https://doi.org/10.1127/0941-2948/2005/0048

Gilmore, C. K., Barrett, S. R. H., Koo, J., & Wang, Q. (2013). Temporal and spatial variability in the aviation NO_x-related O_3 impact. *Environmental Research Letters*, *8*(3), 034027. https://doi.org/10.1088/1748-9326/8/3/034027

Grobler, C., Wolfe, P. J., Dasadhikari, K., Dedoussi, I. C., Allroggen, F., Speth, R. L., Eastham, S. D., Agarwal, A., Staples, M. D., Sabnis, J., & Barrett, S. R. H. (2019). Marginal climate and air quality costs of aviation emissions. *Environmental Research Letters*, *14*(11), 114031. https://doi.org/10.1088/1748-9326/ab4942

Lee, D. S., Fahey, D. W., Skowron, A., Allen, M. R., Burkhardt, U., Chen, Q., Doherty, S. J., Freeman, S., Forster, P. M., Fuglestvedt, J., Gettelman, A., De León, R. R., Lim, L. L., Lund, M. T., Millar, R. J., Owen, B., Penner, J. E., Pitari, G., Prather, M. J., … Wilcox, L. J. (2021). The contribution of global aviation to anthropogenic climate forcing for 2000 to 2018. *Atmospheric Environment*, *244*, 117834. https://doi.org/10.1016/j.atmosenv.2020.117834

Lund, M. T., Aamaas, B., Berntsen, T., Bock, L., Burkhardt, U., Fuglestvedt, J. S., & Shine, K. P. (2017). Emission metrics for quantifying regional climate impacts of aviation. *Earth System Dynamics*, *8*(3), 547–563. https://doi.org/10.5194/esd-8-547-2017

Olsen, S. C., Wuebbles, D. J., & Owen, B. (2013). Comparison of global 3-D aviation emissions datasets. *Atmospheric Chemistry and Physics*, *13*(1), 429–441. https://doi.org/10.5194/acp-13-429-2013

Reynolds, T. (2008, September 14). Analysis of lateral flight inefficiency in global air traffic management. *The 26th Congress of ICAS and 8th AIAA ATIO*. The 26th Congress of ICAS and 8th AIAA ATIO, Anchorage, Alaska. https://doi.org/10.2514/6.2008-8865

Teoh, R., Schumann, U., & Stettler, M. E. J. (2020). Beyond contrail avoidance: Efficacy of flight altitude changes to minimize contrail climate forcing. *Aerospace*, *7*(9), 121. https://doi.org/10.3390/aerospace7090121